

# CFD Analysis of Fluid Flow and Heat Transfer in Two Phase Flow Microchannels

Pramod kumar<sup>1</sup>, M.R.Nagraj<sup>2</sup>

<sup>1</sup>\*PG Student, Thermal power Engineering, PDA College of Engineering, Gulbarga-585102, Karnataka

Professor <sup>2</sup>Department of Mechanical Engineering, PDA College of Engineering, Gulbarga-585102, Karnataka (INDIA)

---

## Abstract

This paper presents the computational fluid dynamic Analysis of fluid flow and heat transfer in two phase flow microchannel. In this paper void fraction, pressure drop and heat transfer coefficient is described. The microchannel is of 0.5mm hydraulic diameter and a length of 100mm. The first simulation is done on mass flow rate ranges from 0.1 g/s to 0.4g/s and the 1000  $W/m^2$  is the uniform heat flux along the length of the microchannel. The temperature at the inlet is the saturation temperature of 30°C and the pressure at the inlet is atm pressure. The second simulation is done on mass flow rate of 0.5 g/s to 0.8 g/s and 3000  $W/m^2$  is the uniform heat flux along the length of the microchannel. The temperature at the inlet is again the saturation temperature of 35°C and atm pressure. The coolant used on both the simulation is the refrigerant R-134a. The simulation results predict the void fraction, pressure drop and heat transfer coefficient in a two-phase flow microchannel.

Keywords. Microchannel, two phase flow, void fraction, pressure drop and heat transfer coefficient etc.

---

## 1. Introduction

Two-phase micro-channel heat sinks are devices that feature flow boiling of a liquid coolant through parallel channels having a hydraulic diameter of 10–1000  $\mu m$ . These devices are ideally suited for high-heat-flux dissipation from small surface areas in a broad range of emerging technologies. The combination of small flow passage area and flow boiling produce very high heat transfer coefficients with minimal flow rate and overall coolant inventory requirements, and provide better stream-wise temperature uniformity than single-phase micro-channel heat sinks. Deployment of two-phase micro-channel technology requires a comprehensive fundamental understanding of virtually all hydrodynamic and thermal aspects of phase change in small channels. The ability to accurately predict pressure drop and flow boiling heat transfer for a given micro-channel geometry and operating conditions is of paramount importance to both the design and performance assessment of a micro-channel heat sink. Because the interest in implementing these devices is fairly recent, brought about mostly by thermal intended to aid in the design of compact heat exchangers. The hydraulic diameter for mini-channels is typically on the order of a few millimeters, which is several times larger than those found in micro-channel heat sinks. Nonetheless, the findings from mini-channel studies are useful at pointing out fundamental differences in flow boiling behavior as hydraulic diameter is reduced from macro-scale (several centimeters) to the mini-channel scale, and progressively to micro-channel. Electronic components dissipate more and more heat due to their increasing working capacities. irreversible

damages occur when their internal temperature reach 150°C. For this, the internal temperature of these electronic components is limited to about 100°C with a surface temperature of 85°C due to the temperature gradient. For a specific example, PC chips have a maximum surface working temperature of about 67°C. Thus, effective heat dissipation is required.

Micro or mini heat spreaders are used in the interest of providing higher cooling capability for microtechnologies. They are characterized by high heat flux dissipation and a better heat transfer coefficient compared to conventional processes. Higher effectiveness means, for an identical power, a reduction of size and cost. Compactness also reduces the amount of charge of the fluid, which has also a direct positive impact on safety and environment. However the negative point is possibly a higher pressure drop related to the micro or mini flow channels.

The thermal performance of heat spreaders using micro or mini channels are not yet well understood, for this the fundamentals of two phase heat transfer in microchannels are being studied. Many heat transfer design methods exist for refrigerant vaporization inside macrochannels, but these have been found not to be suitable to the small dimensions found in microchannels due to small scale phenomena. Therefore, research is underway to investigate these small scale phenomena and to develop new microchannel design methods.

Following are the researchers who worked on two phase flow microchannels.

**B. Agostini and A. Bontemps. [1]** This article presents an experimental study of ascendant forced flow boiling in mini-channels with refrigerant R134a. A flat aluminium multi-port extruded tube composed of 11 parallel rectangular channels (3.28 mm × 1.47 mm) with hydraulic diameter of 2.01 mm was used. Mass flux ranged from 90 to 295 kg/m<sup>2</sup> s and heat flux from 6.0 to 31.6 kW/m<sup>2</sup>. Two working pressures, 405 and 608 kPa were tested. Inlet subcooling varied from 1 to 17 K. Heat transfer was found to be greater than that previously reported in the literature for conventional tubes, while dry-out occurred at low qualities.

**Sarizawa et al [2]** Gas-liquid two-phase flow patterns are visualized with a microscope for air-water flow in circular tubes of 20, 25 and 100 μm i.d. and for steam-water flow in a 50 μm i.d. circular tube. The superficial velocities cover a broad range of  $J_L=0.003-17.52$  m/s and  $J_G=0.0012-295.3$  m/s for air-water flows.

**Suo and Griffith [3]** the adiabatic flow of two phases, gas and liquid, has been studied in horizontal tubes of capillary diameter. The flow has been studied primarily in the regime where the gas flows as long bubbles separated from the wall of the tube by a liquid film and from each other by slugs of liquid.

**Lazarek and black [4]** The local heat transfer coefficient, pressure drop, and critical heat flux have been measured for saturated boiling of R-113 in a round tube with an internal diameter 0.31 cm, and heated lengths of 12.3 and 24.6 cm. The experiments include vertical, co-current up flow and down flow configurations. A correlation for the local heat transfer coefficient is presented which expresses the Nusselt number as a function of the liquid Reynolds number and boiling number. Pressure drop data for frictional, spatial acceleration and 180° bend losses were successfully correlated by employing slight modifications to commonly accepted two-phase techniques reported in the literature.

**Mashima and Habiki et al [5]** Flow regime, void fraction, rise velocity of slug bubbles and frictional pressure loss were measured for air-water flows in capillary tubes with inner diameters in the range from 1 to 4 mm. Although some flow regimes peculiar to capillary tubes were

observed in addition to commonly observed ones, overall trends of the boundaries between flow regimes were predicted well by Mishima-Ishii's model. The void fraction was correlated well by the drift flux model with a new equation for the distribution parameter as a function of inner diameter.

**Kew and Cornwell [6]** this paper describes aspects of the work relating to boiling in single, small-diameter tubes as part of a study of compact two-phase heat exchangers. In order to realize the energy-saving potential of compact heat exchangers for evaporating duties it is necessary to establish design procedures. A test facility was commissioned which was used to measure pressure drop and boiling heat transfer coefficients for R141b flowing through tubes 500 mm long with diameters of 1.39–3.69 mm. Established correlations predicted the heat transfer coefficients reasonably well for the largest tube but performed badly when applied to the smaller tubes.

## 2. Geometry and meshing

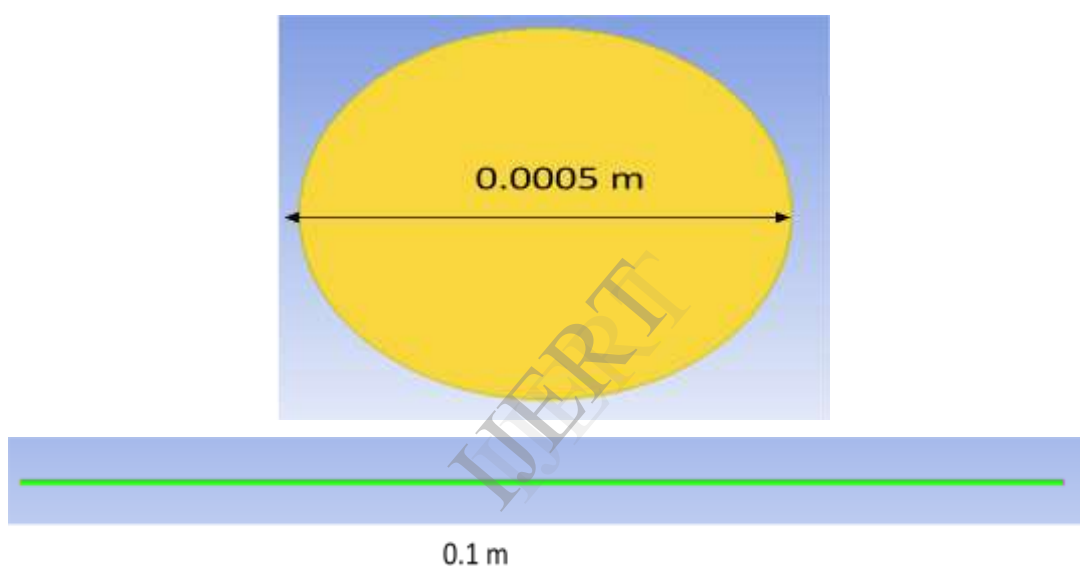


Figure 1 shows the geometry of the microchannel of 0.0005 m (0.5mm) diameter and 0.1 m (100 mm) length.

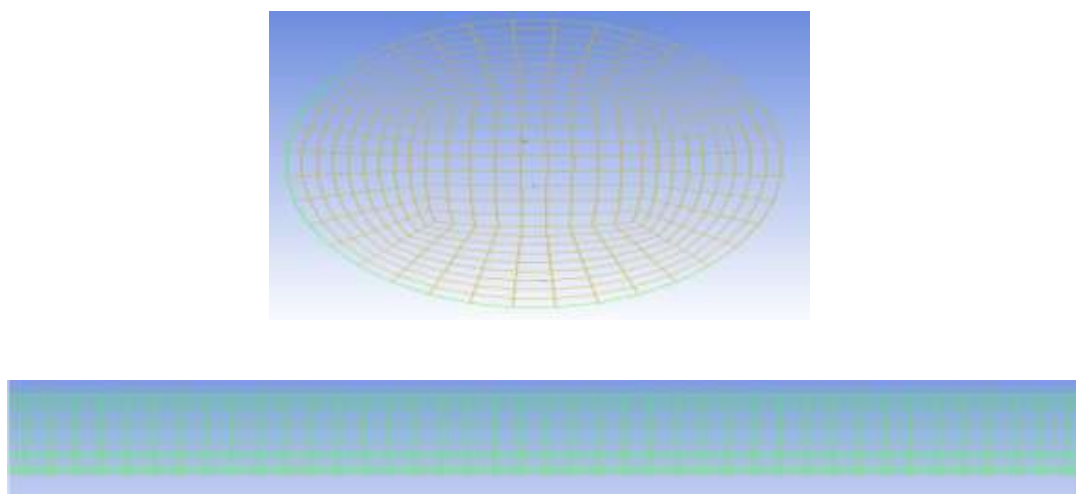


Figure 2 shows the orthogonal meshing of the microchannel.

### 3. Governing equations

#### Two phase flow modeling equations.

A large number of flows encountered in nature and technology are a mixture of phases. Physical phases of matter are gas, liquid, and solid, but the concept of phase in a multiphase flow system is applied in a broader sense. In multiphase flow, a phase can be defined as an identifiable class of material that has a particular inertial response to and interaction with the flow and the potential field in which it is immersed. Currently there are two approaches for the numerical calculation of multiphase flows: the Euler-Lagrange approach and the Euler-Euler approach.

#### Euler-Lagrange approach

The Lagrangian discrete phase model in ANSYS FLUENT follows the Euler-Lagrange approach. The fluid phase is treated as a continuum by solving the Navier-Stokes equations, while the dispersed phase is solved by tracking a large number of particles, bubbles, or droplets through the calculated flow field. The dispersed phase can exchange momentum, mass, and energy with the fluid phase.

#### Euler-Euler approach

In the Euler-Euler approach, the different phases are treated mathematically as interpenetrating continua. Since the volume of a phase cannot be occupied by the other phases, the concept of phase volume fraction is introduced. These volume fractions are assumed to be continuous functions of space and time and their sum is equal to one. In ANSYS FLUENT, three different Euler-Euler multiphase models are available: the volume of fluid (VOF) model, the mixture model, and the Eulerian model. The VOF model is a surface-tracking technique applied to a fixed Eulerian mesh. It is used for two or more immiscible fluids where the position of the interface between the fluids is of interest. In the VOF model, a single set of momentum equations is shared by the fluids, and the volume fraction of each of the fluids in each computational cell is tracked throughout the domain. The mixture model is designed for two or more phases (fluid or particulate). As in the Eulerian model, the phases are treated as interpenetrating continua. The mixture model solves for the mixture momentum equation and prescribes relative velocities to describe the dispersed phases.

#### Volume of Fluid (VOF) Model

The VOF formulation in ANSYS FLUENT is generally used to compute a time-dependent solution, but for problems in which concerned are only with a steady-state solution; it is possible to perform a steady-state calculation.

#### Volume Fraction Equation

The tracking of the interface(s) between the phases is accomplished by the solution of a continuity equation for the volume fraction of one (or more) of the phases. For the  $q^{th}$  (fluid's volume fraction) phase, this equation has the following form:

$$\frac{1}{\rho_q} \left[ \frac{\partial}{\partial t} (\alpha_q \rho_q) + \nabla \cdot (\alpha_q \rho_q \vec{u}_q) \right] = S_{\alpha_q} + \sum_{p=1}^n (m_{pq} - m_{qp}) \quad (2.13)$$

Where  $m_{qp}$  is the mass transfer from phase q to phase p and  $m_{pq}$  is the mass transfer from phase p to

phase  $q$ . By default, the source term on the right-hand side of Eq (2.13)  $S_{\alpha_p}$  is zero, but we can specify a constant or user-defined mass source for each phase. The volume fraction equation will not be solved for primary phase; the primary-phase volume fraction will be computed based on the following constraint:

$$\sum_{q=1}^n \alpha_q = 1 \quad (2.14)$$

### Material Properties

The properties appearing in the transport equations are determined by the presence of the component phases in each control volume. In a two-phase system, for example, if the phases are represented by the subscripts 1 and 2, and the mixture density in each cell is given by

$$\rho = \alpha_2 \rho_2 + (1 - \alpha_2) \rho_1 \quad (2.15)$$

In general, for  $n$  phase system, the volume-fraction-averaged density takes on the following form:

$$\rho = \sum \alpha_q \rho_q \quad (2.16)$$

All other properties (e.g., viscosity) are also computed in this manner.

### Momentum Equation

A single momentum equation is solved throughout the domain, and the resulting velocity field is shared among the phases. The momentum equation, shown below, is dependent on the volume fractions of all phases through the properties  $\rho$  and  $\alpha$

$$\frac{\partial}{\partial t}(\rho \vec{v}) + \nabla \cdot (\rho \vec{v} \vec{v}) = -\nabla p + \nabla \cdot [\mu (\nabla \vec{v} + \nabla \vec{v}^T)] + \rho \vec{g} + \vec{F} \quad (2.17)$$

One limitation of the shared-fields approximation is that in cases where large velocity differences exist between the phases, the accuracy of the velocities computed near the interface can be adversely affected.

### Energy Equation

The energy equation, also shared among the phases, is shown below:

$$\frac{\partial}{\partial t}(\rho E) + \nabla \cdot (\vec{v}(\rho E + p)) = \nabla \cdot (k_{eff} \nabla T) + S_h \quad (2.18)$$

The VOF model treats energy,  $E$  and temperature,  $T$  as mass-averaged variables:

$$E = \frac{\sum_{q=1}^n \alpha_q \rho_q E_q}{\sum_{q=1}^n \alpha_q \rho_q} \quad (2.19)$$

Where Eq for each phase is based on the specific heat of that phase and the shared temperature. The properties  $\rho$  and  $k_{eff}$  (effective thermal conductivity) are shared by the phases. The source term,  $S_h$ , contains contributions from radiation, as well as any other volumetric heat sources.

### Mixture Model

The mixture model is a simplified multiphase model that can be used in different ways. The mixture model allows us to select granular phases and calculates all properties of the granular phases. This is applicable for liquid-solid flows.

### Continuity Equation

$$\frac{\partial}{\partial t}(\rho_m) + \nabla \cdot (\rho_m \vec{u}_m) = 0 \quad (2.20)$$

Where  $u_m$  is the mass-averaged velocity:

$$\vec{u}_m = \frac{\sum_{k=1}^n \alpha_k \rho_k \vec{u}_k}{\rho_m} \quad (2.21)$$

Where  $\rho_m$  is the mixture density:

$$\rho_m = \sum_{k=1}^n \alpha_k \rho_k \quad (2.22)$$

$\alpha_k$  is the volume fraction of phase  $k$

### Momentum Equation

Momentum equations for all phases. It can be expressed as the momentum equation for the mixture can be obtained by summing the individual:

$$\begin{aligned} \frac{\partial}{\partial t}(\rho_m \vec{u}_m) + \nabla \cdot (\rho_m \vec{u}_m \vec{u}_m) = & -\nabla p + \nabla \cdot [\mu_m (\nabla \vec{u}_m + \nabla \vec{u}_m^T)] \\ & + \rho_m \vec{g} + \vec{F} + \nabla \cdot \left( \sum_{k=1}^n \alpha_k \rho_k \vec{u}_{dr,k} \vec{u}_{dr,k} \right) \end{aligned} \quad (2.23)$$

Where  $n$  is the number of phases,  $\vec{F}$  is a body force, and  $\mu_m$  is the viscosity of the mixture (2.24) defined as

$$\mu_m = \sum \alpha_k \mu_k \vec{u}_{dr,k}$$

is the drift velocity for secondary phase  $k$  :

$$\vec{u}_{dr,k} = \vec{u}_k - \vec{u}_m \quad (2.25)$$

## Energy Equation

The energy equation for the mixture takes the following form:

$$\frac{\partial}{\partial t} \sum_{k=1}^n (\alpha_k \rho_k E_k) + \nabla \cdot \sum_{k=1}^n (\alpha_k \vec{v}_k (\rho_k E_k + p)) = \nabla \cdot (k_{eff} \nabla T) + S_E \quad (2.26)$$

Where  $k_{eff}$  is the effective conductivity ( $\sum \alpha_k (k_k + k_t)$ ), where  $k_t$  is the turbulent thermal conductivity, defined according to the turbulence model being used). The first term on the right-hand side of Eq. 2.26 represents energy transfer due to conduction.  $S_E$  includes any other volumetric heat sources. In Eq. 2.26

$$E_k = h_k - \frac{p}{\rho_k} + \frac{v_k^2}{2} \quad (2.27)$$

For a compressible phase, and  $E_k = h_{kv}$  for an incompressible phase, where  $h_k$  is the sensible enthalpy for phase k.

## Volume Fraction Equation for the Secondary Phases

From the continuity equation for secondary phase  $p$ , the volume fraction equation for secondary phase  $p$  can be obtained:

$$\frac{\partial}{\partial t} (\alpha_p \rho_p) + \nabla \cdot (\alpha_p \rho_p \vec{v}_m) = -\nabla \cdot (\alpha_p \rho_p \vec{v}_{dr,p}) + \sum_{q=1}^n (m_{qp} - m_{pq}) \quad (2.28)$$

## 4. Results and Discussion

The present project work is on two phase flow microchannel in which the computational fluid dynamics simulations is carried out on different mass flow rate and uniform heat flux in order to get high heat transfer coefficient and high heat removal capability for a given mass flow rate of a coolant. For the first modification, the mass flow rates are 0.1, 0.2, 0.3 and 0.4 g/s and uniform heat flux of  $1000 \text{ W/m}^2$ . For the second modification, the mass flow rates are 0.5, 0.6, 0.7 and 0.8 g/s and uniform heat flux is  $3000 \text{ W/m}^2$ . In this project the simulation is carried on vapour velocity v/s vapour quality, mass flow rate v/s pressure drop and mass flow rate v/s heat transfer coefficient. As from the graph pressure drop versus mass flow rate, pressure drop is high at 0.1 g/s and decreases with increase in mass flow rate up to 0.4 g/s. this is due to the fact that the vaporization takes place at very early stage and the vapour gets dried out, this causes the increase in pressure at 0.1 g/s and 0.5 g/s. wall heat transfer coefficient versus mass flow rate shows the increase in wall heat transfer coefficient due to the increase in vapour quality across the microchannel. The graph of vapour velocity versus vapour quality shows that the vapour velocity



is dependent on vapour quality which yields increase in vapour quality and increase in wall heat transfer coefficient.

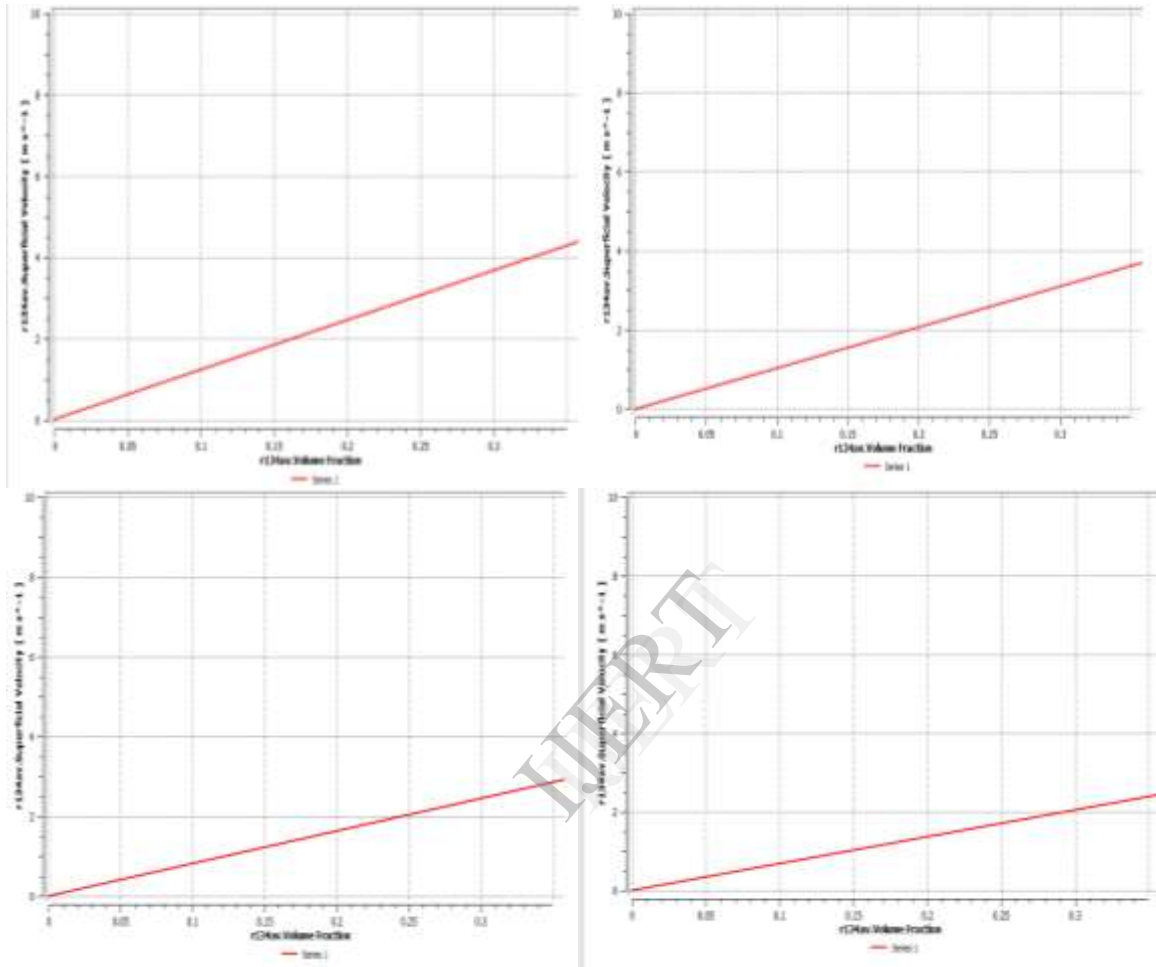
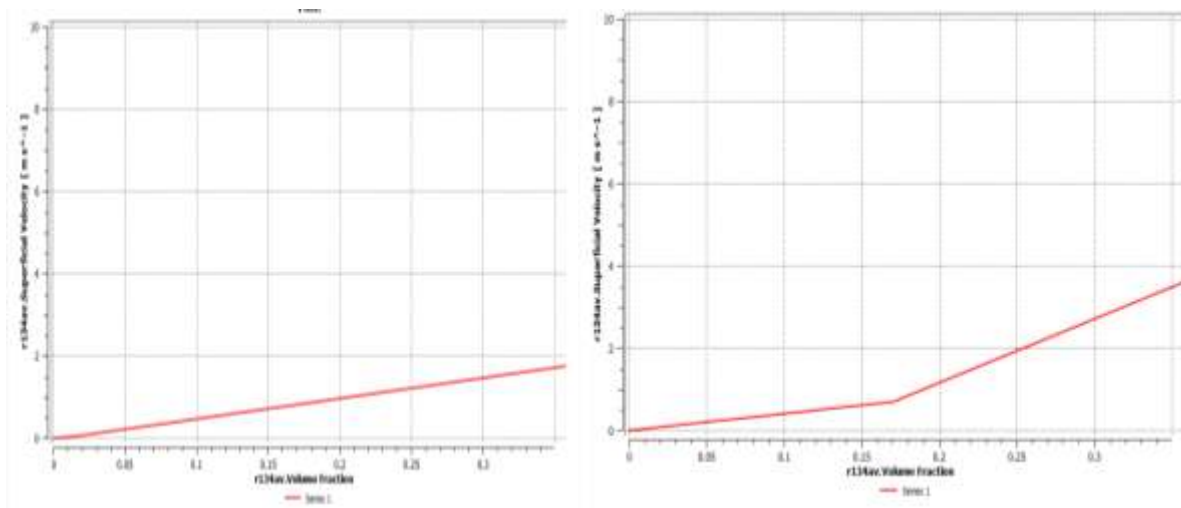


Figure 3 show the four graphs of vapour velocity v/s vapour quality of mass flow rates 0.1, 0.2, 0.3 and 0.4 g/s.





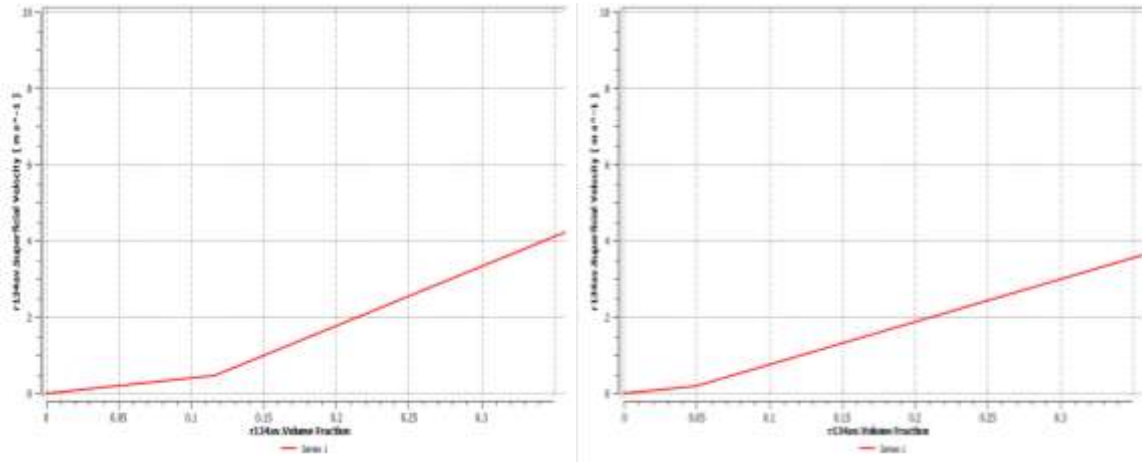


Figure 4 show the four graphs of vapour velocity v/s vapour quality of mass flow rates 0.5, 0.6, 0.7 and 0.8 g/s.

**Pressure drop and heat transfer coefficient**

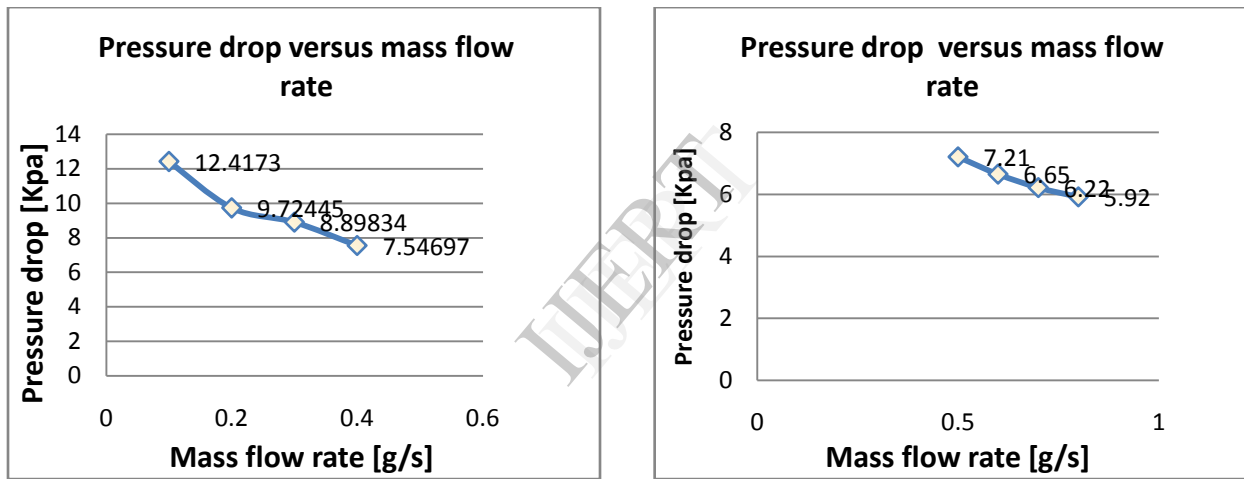


Figure 5 show the two graphs of mass flow rate of 0.1 to 0.4 g/s v/s pressure drop and 0.5 to 0.8 g/s v/s pressure drop. Second graph.

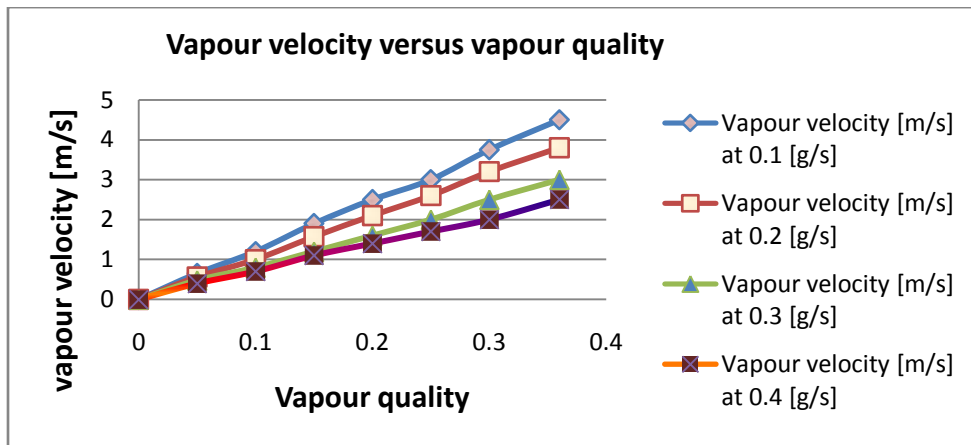


Figure 6 shows the CFD simulated graph for vapour velocity versus vapour quality for mass flow rate ranges from 0.1 g/s to 0.4 g/s.

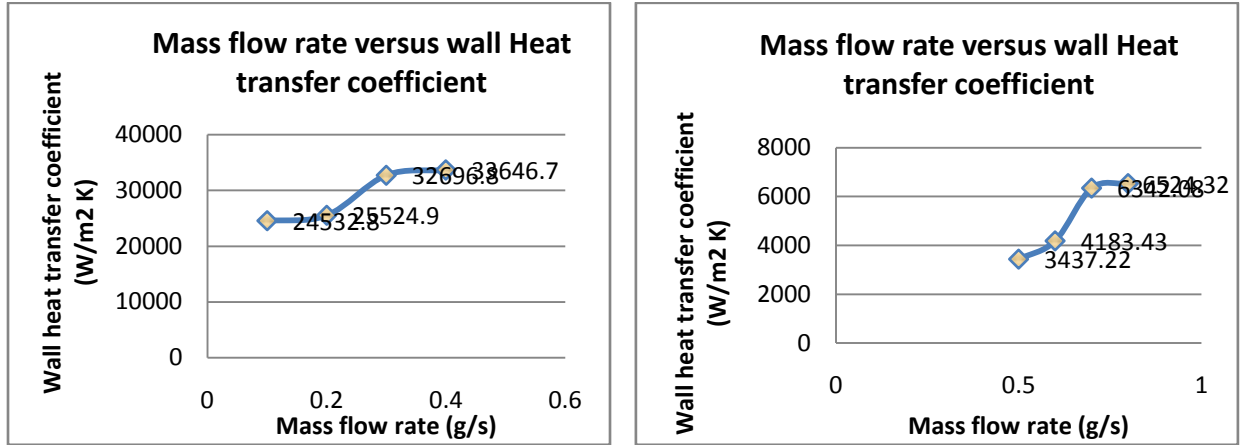
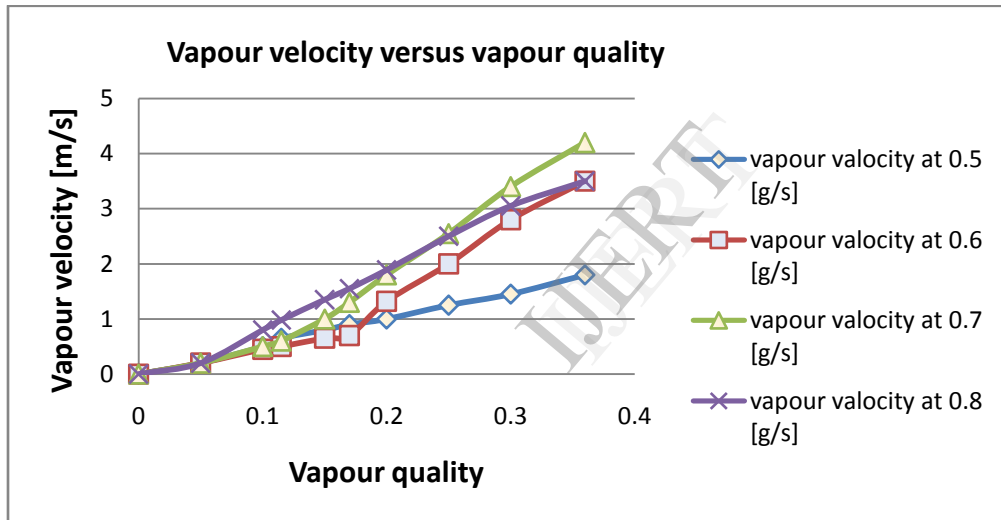


Figure 5 show the two graphs of mass flow rate of 0.1 to 0.4 g/s versus wall heat transfer and mass flow rate of 0.5 to 0.8 g/s versus wall heat transfer .second graph.



## 6. Conclusions

Computational fluid dynamic analysis of fluid flow and heat transfer in two phase flow microchannel using the refrigerant R-134a is made using ANSYS 13 SOLVER. Geometry and meshing of the microchannel is done in ICEM CFD. Boundary conditions are given at CFX PRE and simulation is done on CFX SOLVER and respective calculations are calculated in CFX POST. The simulation is done on different mass flow rates ranging from 0.1 to 0.8 g/s with uniform heat flux  $1000 \text{ W/m}^2$  and  $3000 \text{ W/m}^2$ . The graph of pressure drop versus mass flow rate, wall heat transfer coefficient versus mass flow rate and vapour velocity versus vapour quality were calculated and plotted.

With regards to the computational simulation in the present study the following conclusions can be drawn:

- The graph of pressure drop versus mass flow rate predicts that the pressure drop is high at low mass flow rate i.e. at 0.1 g/s due to the vaporisation takes place inside the microchannel vary early. The bubbles inside the channel gets heated up and dry vapour is formed. This should not happen because this affects the wall heat transfer coefficient and heat removal capacity of the microchannel.
- Vapour velocity is dependent on vapour quality, mass flow rate and the saturation temperature of the fluid. It is observed from the graph that vapour velocity is maximum when the mass flow is high. As the mass flow decreases the vapour velocity decreases.
- Heat transfer coefficient is dependent on saturation temperature of the fluid and mass flow rate of the fluid inside the microchannel. From the graph the heat transfer coefficient increases with increase in mass flow rate due the fact that at high flow rate heat flux increase and formation of bubbles starts and boiling takes place.

## 7. References

- [1] B. Agostini and A. Bontemps. Vertical flow boiling of refrigerant R-134a in small channels. *Intjhhf*, 26:296-306, 2005.
- [2] A Srizawa, Z. Feng, and Z. Kawara. Two-phase flow in microchannels. *Exp. Thermal fluid sci.*, 26:703-714, 2002.
- [3] M. Suo and P. Griffith. Two-phase flow in capillary tubes. *J. Basic Engineering*, pages 576-582, 1964.
- [4] Lazarek G.M., Black S.H., 1982, Evaporative heat transfer, pressure drop and critical heat flux in a small vertical tube with R-113, *Int. J Heat Mass Transfer*, Vol. 25, No. 7, pp. 945-960.
- [5] K. Mishima and T. Hibikil some characteristics of air-water flow in small diameter verticles tubes. *Int. J. Multiphase Flow*, 22:703-712, 1996.
- [6] K. Cornwell and P. A. Kew. Boiling in small channels. In P. Pilavachi, editor, *Proceedings of CEC conference on Energy Efficiency in process Technology*, pages 624-638, Athens, Greece, 1992. Elsevier.
- [7] K. A triplett, S. M. Ghiaasiaan, S I. Abdel-khalik, A. LeMouel, and B. N. McCord. Gas-liquid two-phase flow in microchannels part II: void fraction and pressure drop. *Int. J. Multiphase Flow*, 25:395-410, 1999.
- [8] K. A triplet, S. M. Ghiaasiaan, S I. Abdel-khalik, and D. L. Sadowski. Gas-liquid two-phase flow in microchannels part i: two- phase flow patterns. *Int. J. Multiphase Flow*, 25:377-394, 1999.
- [9] A. Kawahara, P. M. Y. Chung, and M. Kawaji, Investigation of flow pattern, void fraction and pressure drop in a microchannel. *Int. J. Multiphase Flow*. 28:1411-1435, 2002.p
- [10] J. W. Coleman and S. Garimella. Characterization of two-phase flow patterns in small diameter round and rectangular tubes. *Int. J Heat Mass Transfer*, 42:2869-2881, 1999.
- [11] J. W. Coleman and S. Garimella. Two-phase flow regime transition in microchannel tubes:

the effect of hydraulic diameter. In Proceedings of the ASME Heat Transfer Division, volume 4, pages 71-83, 2000.

[12] H. J. Lee and S. Y. Lee. Pressure drop correlation for two-phase flow within horizontal rectangular channels with small heights. *Int. J. Multiphase Flow*, 27:783-796, 2001.

[13] J Lee and I. Mudawar. Two-phase in high heat flux microchannel heat sink for refrigeration cooling applications: part i-pressure drop charecteristics. *Int. J. Heat Mass Transfer*, 48:928-940, 2005.

IJERT